*Original Research Article*

# Quantum chemical and Experimental Techniques for Evaluation of Expired *GlucoredForte* Drugs as Corrosion Inhibitor for mild Steel in HCl solution


## ABSTRACT

The basic corrosion protection technology can lead to expensive problems not only financial but also with respect to safety as well if not properly checked. The present work investigates the corrosion inhibition of mild steel using an expired *GlucoredForte* drug in 2 M HCl solution. The inhibitive properties of mild steel in 2 M HCl solution were evaluated at various temperature range of 30°C – 50°C using weight loss measurements. The expired GlucoredForte drug showed efficiency of 85.7% at concentration of 300ppm. The negative values of Gibb's free energy ($\Delta G^{o}_{ads}$) ranged from -14.52 kJ/mol to -22.57 kJ/mol indicating spontaneous adsorption of the inhibitors on a mild steel surface, and the adsorption mechanism is physisorption. The positive values of ΔH° reflect the endothermic behavior of the adsorption of the studied inhibitor on the mild steel surface. The negative values for entropy imply that the adsorption process is accompanied by a decrease in entropy.The obtained results showed that inhibition efficiency increased with increase in concentration of inhibitors and immersion time and decreased with increase in temperature. Temkin adsorption isotherm model was employed to determine the equilibrium of adsorption for the inhibiting process in the inhibitors. The observable effect of Glibenclamide molecule is strengthened by the presence of heteroatoms such as Nitrogen and Oxygen, as well as the presence of π-bonds in the aromatic rings which facilitate surface interaction.



*Keywords: GlucoredForte, mild steel, enthalpy, entropy, drug*


## 1. INTRODUCTION

Negligence of the basic corrosion protection technology can lead to expensive problems not only financial but also with respect to safety as well. This is why anti-corrosion techniques are of much importance and they can be determined at two levels: prevention at the stage of design, the "cure" stage after corrosion has set in. These include engineering design, anodic protection, lining, cathodic protection and corrosion inhibition. Corrosion control of metals is of technical, economic, environmental, and aesthetical importance. The use of inhibitors is one of the best options of protecting metals and alloys against corrosion [3].

Drugs is one of the most famous chemical materials of every daily and continuous use in our homes, the expired drugs considered as the dangerous materials in the environment cause the death of more than 2000 child's every year, in some countries the expired drugs were wasted in the holes in a deserts which leading to the pollution of the underground water by harmful materials. All this observations take the attentions of Reda Abdel Hameed to search about the new applications for the expired drugs, the using of the expired medicinal drugs as corrosion inhibitors for the metals and alloys was introduced at the first time by Abdelhameed 2009 and 2011, [16,17] when he applied the expire drugs ranitidine as potential nontoxic eco-friendly inhibitor for the corrosion of aluminum in hydrochloric acid solution, his work have been take attention of the another scientists and researchers to evaluate and study many of the expired drugs materials as corrosion inhibitors, Further, the research of unused drugs has been focused on corrosion inhibition of the

steel in different corrosive environments [16-21]. In the last decade the scientific efforts in the field of corrosion inhibition were attended on the eco-friendly and potential nontoxic corrosion inhibitors known as green corrosion inhibitors. The most recent efforts are the use of expired drugs to solve not only the problem of soiled waste accumulations but also to introduce a potential nontoxic inhibitor also to save energy, money consumed in the preparing or sailing a chemical corrosion inhibitor as about of 7 % from the total income were consumed in the protection of metals from the corrosion in many industrial fields. Following the green chemistry concepts, the application of expired drugs in the metallic protections of metals helps in the important green condition. Also, there is no any waste for the process of using drugs as inhibitors as it was taken from the drug market directly to the laboratory, where it was used in their pharmacological form in very few concentrations which is safe for humans and the environment.

The aim of the present work is to recycling of expired Glucored Forte drugs by reusing it as eco-friendly potential nontoxic green inhibitors for corrosion of the mild steel used in manufacturing of petroleum pipe lines. This work shall aid in the assimilation of corrosion mechanisms and minimize corrosion setback. Furthermore, their deformation capacity to adhere to the mild steel surface shall be investigated through the calculations supported by the DFT method of the expired Glucored Forte drug. The structure of one of the organic molecule (Glibenclamide) present in expired Glucored Forte drug is shown in Figure 1.

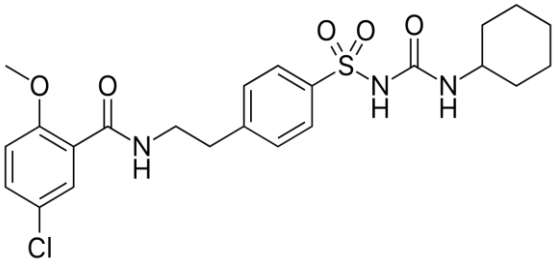


**Figure 1**: Chemical Structure of glibenclamide molecule

## 2. METHODOLOGY

### 2.1 Material preparation

The mild steel sheet was mechanically press-cut into coupons of dimensions 5cm x 4cm. These coupons were used as supplied without further polishing but were however ground with SiC abrasive paper, degreased in ethanol, dried in acetone, weighed and stored in a moisture free desiccator prior to use [20].

### 2.2 Preparation of Solutions

2 M HCl solution was prepared distilled water and a calculated amount of the raw acid solution. The Expired GlucoredForte drug was prepared in concentrations ranging from 100ppm to 300ppm and a solution without the presence of expired GlucoredForte drugs was taken and kept for reference as the Blank solution. Tests were conducted under total immersion conditions in 100 ml of the test solutions maintained at 30-50℃. The pre-cleaned and weighed coupons were immersed totally in beakers containing the test solutions.

### 2.3 Determinations of Corrosion Rates

Weight loss variations were monitored at interval of 2 hours, for a total of 8 hours. After predetermined time, the mild steel specimens immersed were from the test solutions, scrubbed with iron sponge and washed with acetone to remove traces of moisture. The mild steel specimens were then re-weighed. From the change in the weights of the specimens, the corrosion rates were calculated by the formula used in Essien *et al*. [28]:

### 2.4 Molecular modeling

The PM7 Hamiltonian in the MOPAC 2014 software was used in computing semi-empirical parameters for the molecule [15]. The Full optimization was done using molecular mechanics, *Ab initio,* and DFT level [16]. Single point DFT calculations were also carried out using Hyperchem release 8.2 packages. DFT setting (MP2 inclusive) in the package were, Basic set: 321-G, iteration = 50, spin pairing = unrestricted Hartree Fock, convergence limit = 1E-0.05 and Spin

multiplicity = 1 (for zero charge and 2 for +1 and -1 charges). The relation between the inhibition efficiency of this inhibitor and the quantum chemical parameters was considered [17]. The corrosion inhibition mechanisms were studied using quantum chemical calculations, and the probable physical properties were determined to know which could make the inhibition possible.

## 3. RESULTS AND DISCUSSION

3.1 Weight loss studies

To minimize the corrosion of mild steel in the acidic medium, the gravimetric experiment was carried out by using the expired Glucored Forte drug as the inhibitor [15,17]. The weight loss measurement was observed to increase with an increase in time but decrease with an increase in concentrations of the expired Glucored Forte drug (Table 1). A similar trend was observed by many researchers [11,18–23]. Figure 2 showed the weight loss measurements with time at 30° C and related trends were observed at 40°C and 50°C.

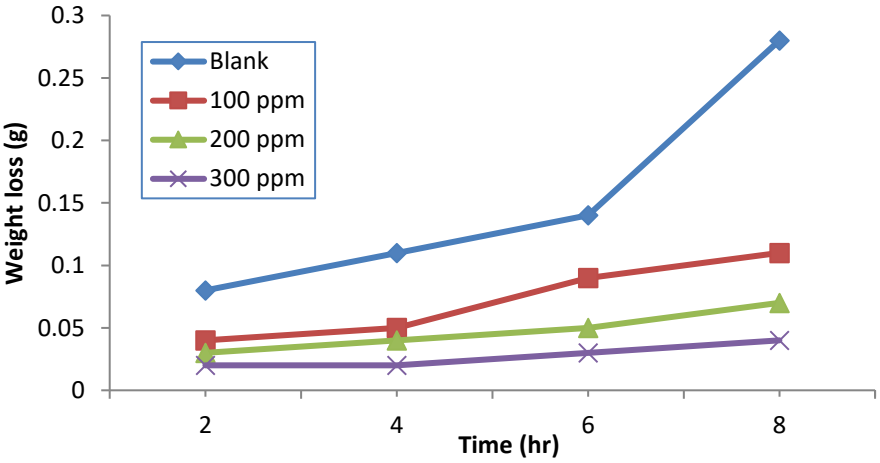


Figure 2: Weight loss versus Time in the absence and presence of different concentrations of expired Glucored Forte at 30℃.

Table 1: Calculated values of corrosion rate (CR), surface coverage (θ) and inhibition efficiency (%I) of mild steel corrosion in different concentration of GLU

| Inhibitor | Conc. (ppm) | 303 K | | | 313 K | | | 323 K | | |
|---|---|---|---|---|---|---|---|---|---|---|
| | | CR (mm/yr) x $10^{-3}$ | θ | I (%) | CR (mm/yr) x $10^{-3}$ | θ | I (%) | CR (mm/yr) x $10^{-3}$ | θ | I (%) |
| GLU | Blank | 1.750 | - | - | 1.380 | - | - | 2.000 | - | - |
| | 100 | 0.686 | 0.608 | 60.8 | 0.563 | 0.592 | 59.2 | 0.930 | 0.532 | 53.2 |
| | 200 | 0.438 | 0.750 | 75.0 | 0.500 | 0.678 | 67.8 | 0.810 | 0.594 | 59.4 |
| | 300 | 0.250 | 0.857 | 85.7 | 0.438 | 0.683 | 68.3 | 0.680 | 0.656 | 65.6 |

The studied compound exhibits corrosion-inhibiting effects at all concentrations reaching a maximum inhibition efficiency of 85.7 % at the optimum concentration of 300 ppm (Table 1). The studied inhibitor was found to be more efficient at 303 K (Table 1). This result corresponds to that of Paul et al. [26], Essien et al. [28] and Dohare et al. [29] which is attributed to partial desorption of the molecules from the Mild Steel surface.

3.2 Effect of temperature

To understudy the temperature dependence of corrosion rates in uninhibited and inhibited solutions, the gravimetric measurements were carried out in the temperature range 303 K – 323 K in the presence of different concentrations of expired Glucored Forte drug in 0.1 M HCl solution [29]. The inhibition efficiencies as a function of concentrations are presented in table 1. The results show that inhibition efficiency increased with the concentration of the inhibitor [30]. Similar behaviour was reported by many researchers [16,29,31–34]. High efficiency of 85.7 % was noticed after 8 h, which points out, that the surface coverage of the substrate by this inhibitor attended an optimum level within 8 h. From the results, the highest concentration of this inhibitor at 303 K gives maximum inhibition efficiency. The results show that inhibition efficiency decreases as the temperature increases indicating the physisorption process as reported by Khaled et al. [19]. From the results, it could be observed that inhibitor concentration increases as the corrosion rate decreases, thus leading to an increase in the inhibition efficiency. The adsorptions of this inhibitor on mild steel surfaces were studied using adsorption isotherms [20,21,35] and Essien et al [28]. Adsorption isotherms gave vital information on the interaction of inhibitor and metal surfaces as observed by Umoren [11]. The degree of surface coverage values (θ) at different inhibitor concentrations in 2 M HCl solutions were assessed from weight loss measurements at 303 K – 333 K and tested graphically for fitting to a suitable adsorption isotherm [22,25,31]. The adsorption isotherm model considered was Temkin isotherm as reported by Obot and Obi-Egbedi [20,23].

The best-fitted straight line in all the adsorption isotherm models considered was in the Temkin isotherm with correlation coefficients (R2) ranging from $0.9952 \geq R2 \geq 1.0000$. The values of molecular interaction parameter 'a' shown in table 2 are negative in all cases which implies attraction in the adsorption layer. A similar result was observed by Obot and Obi-Egbedi [23]. It is obvious from table 2 that, the values of Kads are very low indicating weak interaction between the inhibitor and the mild steel surface which implies the electrostatic interaction (Physisorption) between the inhibitor molecules and the metal surface [36]. The negative values of ΔG°ads indicates spontaneous process [25,30,31].

Table 2: Adsorption parameters from Temkin isotherm for Mild steel coupons in 2 M HCl containing different concentration of expired GlucoredForte drug at 30-50$^{o}$C.

| **Temp. (K)** | **ADSORPTION PARAMETERS** | | | | |
|---|---|---|---|---|---|
| | **Slope** | **Intercept** | **K** | **-∆G(KJ/mol)** | **$R^2$** |
| 303 | 0.125 | 0.49 | 50.40 | 19992.85 | 0.9952 |
| 313 | 0.045 | 0.55 | 202804.96 | 42251.65 | 0.9959 |
| 323 | 0.060 | 0.47 | 2514.93 | 31812.54 | 1.0000 |

The activation energy values in Table 3 indicate that the presence of expired Glucored Forte drug increases the activation energy of the metal dissolution reaction. The adsorption of the studied inhibitors is believed to take place on the higher energy sites and the presence of the inhibitor, which results in the blocking of the active sites, must be related to an increase in the activation energy of mild steel corrosion in the inhibited state [37]. The higher value of Ea in the presence of inhibitors compared to that in its absence and the decrease in the inhibition efficiency (%) with rising in temperature is deduced as an indication of physisorption.

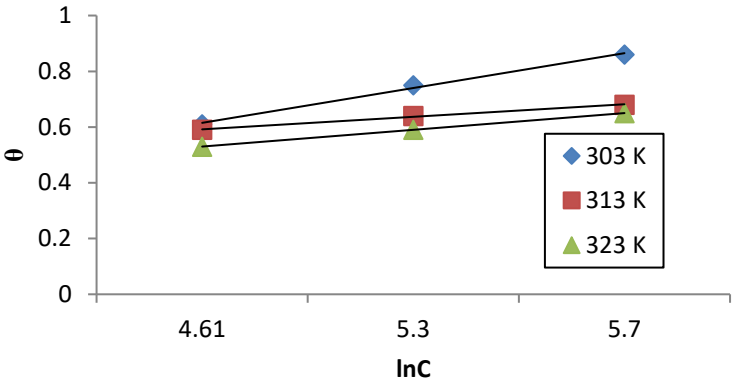


Figure 3: Temkin adsorption isotherm plot as θ versus ln C for Mild steel coupons in 2 M HCl solution containing different concentration of expired GlucoredForte drug.

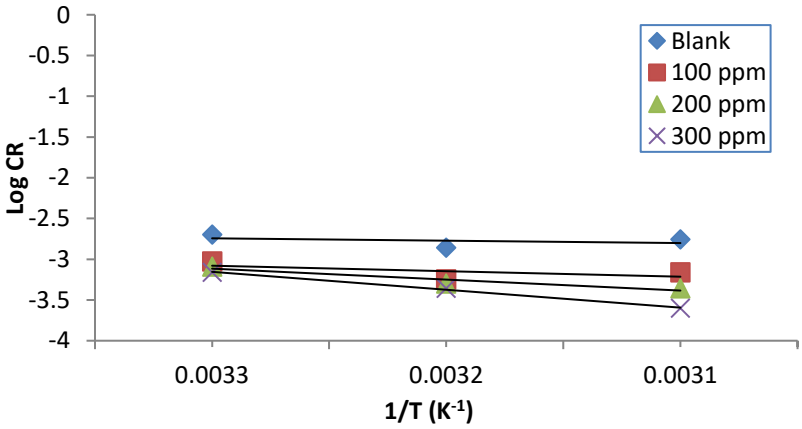


Figure 4: Arrhenius plot as log CR versus 1/T for mild steel coupons in 2 M HCl containing different concentration of expired Glucored Forte drug.

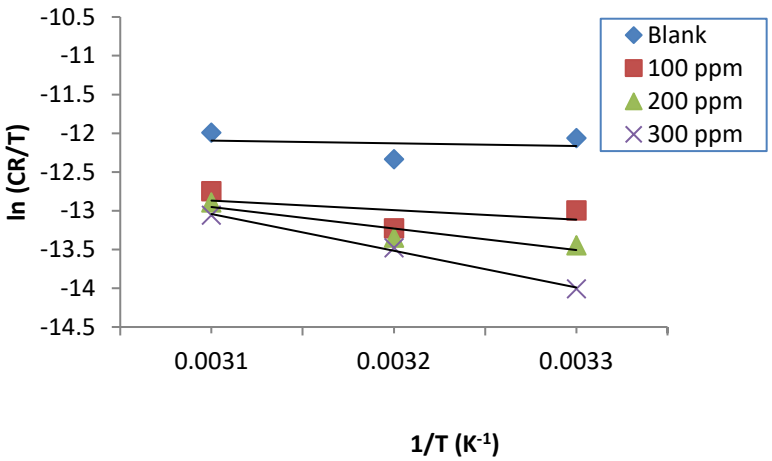


Figure 5: Transition State plot as log (CR/T) versus 1/T for mild steel coupons in 2 M HCl containing different concentration of expired Glucored Forte drug.

The transition state plot is presented in figure 5 [6,31]. The computed values of the activation parameters for the dissolution of mild steel at different temperatures are presented in table 3. Examination of these data in table 3 revealed that the positive values of $\Delta H^o$ reflect the endothermic behavior of the adsorption of the studied inhibitor on the mild steel surface [22,28]. The $\Delta S^o$ values are negative indicating that the adsorption is an endothermic process [22,25,28]. The adsorption between the organic compound in the aqueous phase [org (sol)] and water molecules at the electrode surface [$H_2O$(ads)] is regarded as a quasi-substitution process [30]. Thus, the adsorption of expired Glucored Forte drug is accompanied by the desorption of water molecules from the electrode surface.

Table 3: Activation parameters for Mild steel in 2 M HCl containing different concentrations of expired Glucored Forte drug at 30-50$^o$C.

| expired Glucored Forte drug **Conc. (ppm)** | **ACTIVATION PARAMETERS** | | | |
|---|---|---|---|---|
| | $\Delta H$ (KJ/mol) | $\Delta S$ (J/mol $K^{-1}$) | Ea (KJ/mol) | A x $10^{-3}$ (J/mol $K^{-1}$) |
| Blank | 0.5641 | 85.05 | 0.2893 | 0.0015 |
| 100 | 1.3090 | 79.35 | 1.0235 | 0.0005 |
| 200 | 2.6141 | 79.95 | 2.3080 | 0.0003 |
| 300 | 4.2732 | 80.83 | 3.9392 | 0.0002 |

Consequently, the adsorption process is endothermic and associated with a decrease in entropy of the solute; the same is factual for the solvent. The thermodynamic parameters obtained are the algebraic sum of the adsorption of the expired Glucored Forte drug and the desorption of water molecules [37]. Thus, the increase in entropy is due to the increase in solvent entropy [38]. The negative values for entropy imply that the adsorption process is attended by a decrease in entropy, which is the driving force for the adsorption of expired Glucored Forte drug on the mild steel surface [39].

### 3.3 Global molecular reactivity

The MOPAC 2014 software was used to compute the quantum chemical parameters (Table 4). Similar software has been used by Eddy et. al. [28,40]. The HOMO and LUMO molecular orbitals of the expired Glucored Forte drug are shown in figures 7 and 8 respectively. The blue and maroon orbital represent positive and negative sites of adsorption respectively.

The reactivity of a chemical species can be defined as the difference in energy of the highest occupied molecular orbital (EHOMO) and that of the lowest unoccupied molecular orbital (ELUMO).

Table 4: Molecular properties of Glibenclamide calculated using DFT at the RHF/STO-6G* basis in aqueous phase

| | $E_{HOMO}$ (eV) | $E_{LUMO}$ (eV) | ΔE (eV) | M (debye) | IE (eV) | AE (eV) | χ (eV) | η (eV) | S $(eV)^{-1}$ | ω (eV) | $\Delta E_{b-d}$ (eV) |
|---|---|---|---|---|---|---|---|---|---|---|---|
| GLI | -0.1394 | -0.0467 | -0.0927 | 4716.06 | 0.1394 | 0.0467 | 0.0931 | 0.0464 | 21.58 | -0.0233 | -0.0116 |

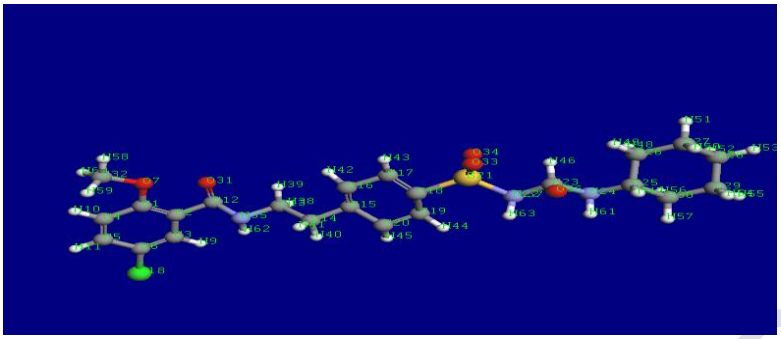

Figure 6: The optimized geometries of the Glibenclamide molecule.

The Glibenclamide molecule was studied theoretically using DFT method at the RHF/STO-6G* level. The electronic parameters of the molecule were correlated with inhibition efficiencies. Quantum chemical parameters like EHOMO, ELUMO, dipole moment, energy gap, ionization energy, electron affinity, etc. were obtained in this study. It could be seen in figure 7, that the HOMO is distributed around the central aromatic ring of benzene and Sulphur atom of the molecule, whereas the LUMO shown in figure 8 is distributed around the central aromatic ring of benzene alone. The high HOMO energy in the molecule confirms the donating ability of the glibenclamide molecule to unoccupied d-orbital of the metal indicating physical adsorption. The low LUMO energy confirms electron accepting tendency from the surface of the metal. Moreover, the gap between LUMO and HOMO (Energy gap, ΔE) energies level of the molecule is a significant factor to be considered because the smaller the energy gap the more efficient the inhibitor.

The smaller the energy gap, the higher reactivity of the chemical species [25,40]. From Table 4, it is obvious that the energy gap, ΔE of the studied inhibitor is 9.78 eV. As a result, the inhibition efficiency of the inhibitor molecule is 71 %. Figures 6 and 7 showed the distribution of HOMO and LUMO of glibenclamide molecule, and it could be seen that the distribution of HOMO and LUMO is mainly located at the oxazole ring, nitrogen, and oxygen atoms in substituent groups. This kind of distribution favors the parallel adsorption of oxazole derivative inhibitor onto the metal surface [6,41]. This implies that the inhibitor molecules donate electrons to the unoccupied d orbital of the Fe atom forming a coordinate bond and the inhibitor molecules accept electrons from the Fe atom to form a back-donating bond [42].

The ionization energy was estimated through the value of EHOMO with Semi-empirical calculations. In this case, two systems, Fe (in mild steel) and inhibitor are brought together, hence, electrons will flow from the lower system with lower electronegativity (inhibitor) to the system with higher electronegativity until the chemical potential becomes equal [15,40]. The trend for the variation of inhibition potentials of the studied oxazole derivative agrees with experimental findings. The hydrophobicity of the actual molecule is accounting for by the substituent Log P. The hydrophobicity of organic molecule increases with decreasing water solubility. In corrosion studies, hydrophobicity is related to the mechanism of formation of the oxide/hydroxide layer on the metal surface (which reduces the corrosion process drastically) [40,43].

The dipole moment is the measured polarity of a polar covalent bond [44]. From table 4, the negative total energy indicates that the studied inhibitor is a very stable molecule and is less prone to be broken apart. The dipole moment of the studied inhibitor is 2.47 Debye which is higher than that of $H_2O$ (1.87 Debye) [28,44]. The high values of dipole moment probably increase the adsorption between the compound and metal surface [49]. Moreover, effective adsorption of the studied molecules on the mild steel surface is enhanced by higher area and volume. Literature discloses that there

are several abnormalities in the correlation involving dipole moment and inhibition efficiency, noting that core-core repulsion (C–C) energy is a quantum chemical parameter that has a tremendous correlation with inhibition efficiency [44].

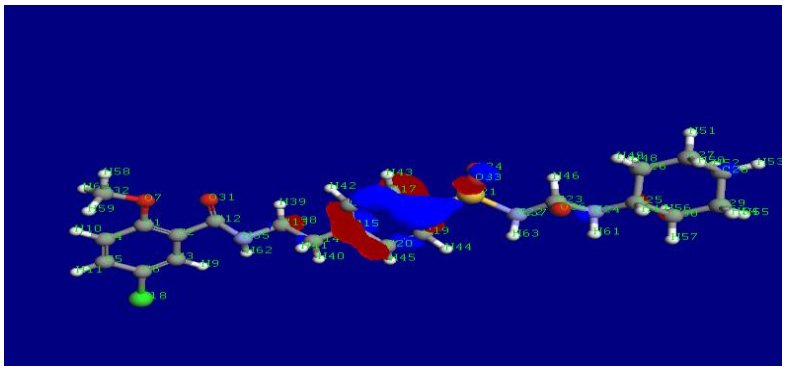

Figure 7: The highest occupied molecular orbital (HOMO) density of Glibenclamide molecule using DFT at the RHF/STO-6G* basis set level

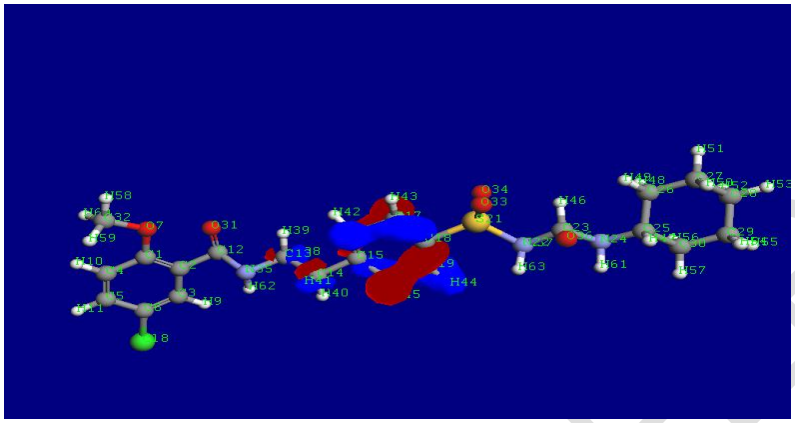

Figure 8: The lowest unoccupied molecular orbital (LUMO) density of Glibenclamide molecule using DFT at the RHF/STO-6G* basis set level

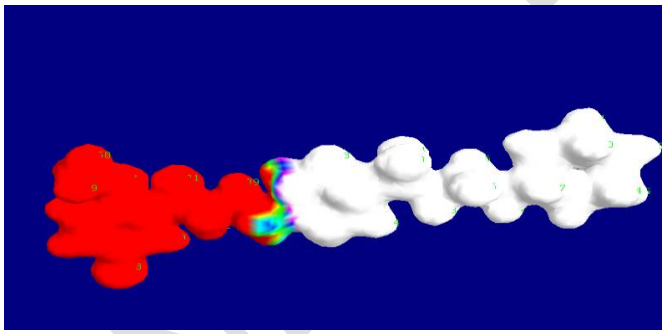

Figure 9: Molecular electrostatic potential-mapped density of Glibenclamide molecule

4.2.4 Mulliken population analysis

The more negative the atomic charges of the absorbed center are, the easier the atom donates electron to the unoccupied d-orbital of metal. Table 5 shows the calculated Mulliken atomic charges for Glibenclamide molecule calculated using DFT at the RHF/STO-6G* basic level.

Table 5: Mulliken atomic charges for the Glibenclamide molecule (GLI)

| Atom | Charge |
|---|---|
| 1C | 4.0000 |
| 2C | 3.9999 |
| 3C | 3.9968 |
| 4C | 3.9999 |
| 5C | 3.9978 |
| 6C | 4.0210 |
| 7O | 6.0000 |
| 8Cl | 4.9830 |
| 9H | 1.0009 |
| 10H | 1.0000 |
| 11H | 1.0006 |
| 12C | 3.9980 |
| 13C | 3.8303 |
| 14C | 2.8051 |
| 15C | 1.1614 |
| 16C | -0.1439 |
| 17C | -3.5616 |
| 18C | -3.9999 |
| 19C | -3.9987 |
| 20C | -2.5104 |
| 21S | -2.0001 |
| 22N | -3.0000 |
| 23C | -4.0000 |
| 24N | -3.0000 |
| 25C | -4.0000 |
| 26C | -4.0000 |
| 27C | -4.0000 |
| 28C | -4.0000 |
| 29C | -4.0000 |
| 30C | -4.0000 |
| 31O | 5.9991 |
| 32C | 4.0000 |
| 33O | -2.0000 |
| 34O | -2.0000 |
| 35N | 4.9850 |
| 36O | -2.0000 |
| 37H | -1.0000 |
| 38H | 0.9944 |
| 39H | 0.9981 |
| 40H | 0.9204 |
| 41H | 0.9361 |
| 42H | 0.4294 |
| 43H | -0.9988 |
| 44H | -1.0018 |
| 45H | 0.1585 |
| 46H | -1.0000 |
| 47H | -1.0000 |
| 48H | -1.0000 |
| 49H | -1.0000 |
| 50H | -1.0000 |
| 51H | -1.0000 |
| 52H | -1.0000 |
| 53H | -1.0000 |

54H -1.0000
55H -1.0000
56H -1.0000
57H -1.0000
58H 1.0000
59H 1.0000
60H 1.0000
61H -1.0000
62H 0.9997
63H -1.0000

The result reveals that most of the Nitrogen atoms, all the Sulphur atoms, a few Hydrogen atoms, some Carbon and Oxygen atoms carry negative Mulliken charge densities, indicating possible sites of adsorption on the surface. Moreover, some carbons atoms and most of the hydrogen atoms carry positive Mulliken charge densities. This indicates the sites in which the molecules could accept electron from the un-occupied d-orbital of the metals as also reported by Eddy et al. [17].

## 4. CONCLUSION

The studied expired drug was found to act as an effective corrosion inhibitor for mild steel in 2 M HCl solution and its inhibition efficiency related with different concentrations and chemical structures. Weight loss measurements were conducted at various temperatures to investigate the corrosion inhibitive behavior of mild steel in 2 M HCl solution. Results demonstrated that inhibitor efficiency had increased with increase in inhibitor concentration and decreased with increase in temperature and immersion time. The adsorption process of the inhibitor on mild steel surface favors a physical adsorption mechanism and is best described by the Temkin adsorption isotherm. Quantum chemical calculations revealed that the studied compound adsorb both as cationic species and as molecular species using oxygen, nitrogen and carbon as its active centers.

## REFERENCES


1. Sastri, V.S. Green corrosion inhibitors: theory and practice, John Wiley & Sons, 2012.

2. El-Etre, A.Y. Inhibition of C-steel corrosion in acidic solution using the aqueous extract of zallouh root, Mater. Chem. Phys. 2008;108 278–282.

3. Le Goff, G. Ouazzani, J. Natural hydrazine-containing compounds: Biosynthesis, isolation, biological activities and synthesis, Bioorg. Med. Chem. 2014; 22 6529–6544.

4. Hosseini, M.G. Ehteshamzadeh, M. Shahrabi, T. Protection of mild steel corrosion with Schiff bases in 0.5 M H2SO4 solution, Electrochim. Acta. 2007; 52 3680–3685.

5. Thoume, A. Elmakssoudi, A. Left, D.B. Benzbiria, N. Benhiba, F. Dakir, M. Zahouily, M. Zarrouk, A. Azzi, M. Zertoubi, M. Amino acid structure analog as a corrosion inhibitor of carbon steel in 0.5 M H2SO4: Electrochemical, synergistic effect and theoretical studies, Chem. Data Collect. 2020; 30 100586.

6. Solomon, M.M. Essien, K.E. Loto, R.T.. Ademosun, O.T Synergistic corrosion inhibition of low carbon steel in HCl and $H_2SO_4$ media by 5-methyl-3-phenylisoxazole-4-carboxylic acid and iodide ions, J. Adhes. Sci. Technol. 2022; 36 1200–1226.

7. Glaser, R. Lewis, M. Wu, Z. Stereochemistry and stereoelectronics of azines. 13. Conformational effects on the quadrupolarity of azines. An ab initio quantum-mechanical study of a lateral synthon, Mol. Model. Annu. 2000; 6 86–98.

8. Yadav, M. Gope, L. Kumari, N. Yadav, P. Corrosion inhibition performance of pyranopyrazole derivatives for mild steel in HCl solution: Gravimetric, electrochemical and DFT studies, J. Mol. Liq. 2016; 216 78–86.

9. El Arrouji, S. Alaoui, K.I. Zerrouki, A. Kadiri, S.E.L. Touzani, R. Rais, Z. Baba, M.F. Taleb, M. Chetouani, A. Aouniti, A. The influence of some pyrazole derivatives on the corrosion behaviour of mild steel in 1M HCl solution, J. Mater. Environ. Sci. 2016; 7 299–309.

10. El Arrouji, S. Karrouchi, K. Berisha, A. Alaoui, K.I. Warad, I. Rais, Z. Radi, S. Taleb, M. Zarrouk, A. New pyrazole derivatives as effective corrosion inhibitors on steel-electrolyte interface in 1 M HCl: Electrochemical, surface morphological (SEM) and computational analysis, Colloids Surfaces A Physicochem. Eng. Asp. 2020; 604 125325.

11. Umoren, S.A. Inhibition of aluminium and mild steel corrosion in acidic medium using Gum Arabic, Cellulose. 2008;15 751–761. https://doi.org/10.1007/s10570-008-9226-4.

12. Umoren, S.A. Synergistic inhibition effect of polyethylene glycol–polyvinyl pyrrolidone blends for mild steel corrosion in sulphuric acid medium, J. Appl. Polym. Sci. 2011; 119, 2072–2084. https://doi.org/10.1002/app.32922.

13. Chauhan, D.S. Quraishi, M.A. Qurashi, A. Recent trends in environmentally sustainable Sweet corrosion inhibitors, J. Mol. Liq. 2021; 326, 115117.

14. Oguzie, E.E. Adindu, C.B. Enenebeaku, C.K. Ogukwe, C.E. Chidiebere, M.A. Oguzie, K.L. Natural products for materials protection: mechanism of corrosion inhibition of mild steel by acid extracts of Piper guineense, J. Phys. Chem. C. 2012;116, 13603–13615. https://doi.org/10.1021/jp300791s.

15. . Ebenso, E.E Isabirye, D.A. Eddy, N.O. Adsorption and quantum chemical studies on the inhibition potentials of some thiosemicarbazides for the corrosion of mild steel in acidic medium, Int. J. Mol. Sci. 2010;11, 2473–2498. https://doi.org/10.3390/ijms11062473.

16. Eddy, N.O. Momoh-Yahaya, H. Oguzie, E.E.Theoretical and experimental studies on the corrosion inhibition potentials of some purines for aluminum in 0.1 M HCl, J. Adv. Res. 2015; 6, 203–217. https://doi.org/10.1016/j.jare.2014.01.004.

17. Eddy, N.O. Ebenso, E.E. Ibok, U.J. Adsorption, synergistic inhibitive effect and quantum chemical studies of ampicillin (AMP) and halides for the corrosion of mild steel in H2SO4, J. Appl. Electrochem. 2010; 40, 445–456. https://doi.org/10.1007/s10800-009-0015-z.

18. Kousar, K. Walczak, M.S. Ljungdahl, T. Wetzel, A. Oskarsson, H. Restuccia, P. Ahmad, E.A. Harrison, N.M. Lindsay, R. Corrosion inhibition of carbon steel in hydrochloric acid: Elucidating the performance of an imidazoline-based surfactant, Corros. Sci. 2021; 180, 109195.

19. Khaled, K.F. Abdel-Rehim, S.S. Sakr, G.B. On the corrosion inhibition of iron in hydrochloric acid solutions, Part I: Electrochemical DC and AC studies, Arab. J. Chem. 2012; 5, 213–218. https://doi.org/10.1016/j.arabjc.2010.08.015.

20. Obi-Egbedi, N.O. Essien, K.E. Obot, I.B. Computational simulation and corrosion inhibitive potential of alloxazine for mild steel in 1M HCl, J. Comput. Methods Mol. Des. 2011; 1, 26–43.

21. Obot, I.B. Obi-Egbedi, N.O. Odozi, N.W. Acenaphtho [1, 2-b] quinoxaline as a novel corrosion inhibitor for mild steel in 0.5 M H2SO4, Corros. Sci. 2010; 52, 923–926. https://doi.org/10.1016/j.corsci.2009.11.013.

22. Tang, L. Li, X. Mu, G. Liu, G. Li, L. Liu, H. Si, Y. The synergistic inhibition between hexadecyl trimethyl ammonium bromide (HTAB) and NaBr for the corrosion of cold rolled steel in 0.5 M sulfuric acid, J. Mater. Sci. 2006; 41, 3063–3069. https://doi.org/10.1007/s10853-006-6987-8.

23. Obot, I.B. Obi-Egbedi, N.O. Fluconazole as an inhibitor for aluminium corrosion in 0.1 M HCl, Colloids Surfaces a Physicochem. Eng. Asp. 2008; 330, 207–212. https://doi.org/10.1016/j.colsurfa.2008.07.058.

24. Njoku, D.I. Onuoha, G.N. Oguzie, E.E. Oguzie, K.L. Egbedina, A.A. Alshawabkeh, A.N. Nicotiana tabacum leaf extract protects aluminium alloy AA3003 from acid attack, Arab. J. Chem. 2019; 12, 4466–4478. https://doi.org/10.1016/j.arabjc.2016.07.017.

25. Jackson, E. Essien, K.E. Experimental and Theoretical Approach of L-Methionine Sulfone (LMS) as corrosion inhibitor for mild steel in HCL Solution, Environment. 2019; 1, 2.

26. Paul, P.K. Yadav, M. Obot, I.B. Investigation on corrosion protection behavior and adsorption of carbohydrazide-pyrazole compounds on mild steel in 15% HCl solution: Electrochemical and computational approach, J. Mol. Liq. 2020; 314, 113513.

27. . Hosseini, S.M.A Salari, M. Jamalizadeh, E. Khezripoor, S. Seifi, M. Inhibition of mild steel corrosion in sulfuric acid by some newly synthesized organic compounds, Mater. Chem. Phys. 2010; 119, 100–105.https://doi.org/10.1016/j.matchemphys.2009.08.029.

28. Essien, K.E. Odiongeyi, A. O. Ekerete, J. B. Okon, E. O. Idongesit, E. O. Nnabuk O. E. Abai, E.J. Corrosion Inhibition Potential of Two Isoxazole Derivatives: Experimental and Theoretical Analyses,. Mater. Environ. Sci., 2022, 13 (8), 928-944.

29. Dohare, P. Quraishi, M.A. Verma, C. Lgaz, H. Salghi, R. Ebenso, E.E. Ultrasound induced green synthesis of pyrazolo-pyridines as novel corrosion inhibitors useful for industrial pickling process: Experimental and theoretical approach, Results Phys. 2019; 13, 102344.

30. Fouda, A.S. Abd El-Aal, A. Kandil, A.B. The effect of some phthalimide derivatives on corrosion behavior of copper in nitric acid, Desalination. 2006; 201 216–223. https://doi.org/10.1016/j.desal.2005.11.030.

31. Jackson, E. Essien, K.E. Okafor, P.C. Experimental and Quantum Studies: A New Corrosion Inhibitor for Mild Steel, *Elixir Corrosion and Dye*, 2016; 90, 37673-3767

32. Verma, C. Saji, V.S. Quraishi, M.A. Ebenso, E.E. Pyrazole derivatives as environmental benign acid corrosion inhibitors for mild steel: experimental and computational studies, J. Mol. Liq. 2020; 298, 111943.

33. Ouchrif, A. Zegmout, M. Hammouti, B. El-Kadiri, S. Ramdani, A. 1, 3-Bis (3-hyroxymethyl-5-methyl-1-pyrazole) propane as corrosion inhibitor for steel in 0.5 M H2SO4 solution, Appl. Surf. Sci. 2005; 252 339–344.

34. El Ouadi, Y. Lamsayah, M. Bendaif, H. Benhiba, F. Touzani, R. Warad, I. Zarrouk, A. Electrochemical and theoretical considerations for interfacial adsorption of novel long chain acid pyrazole for mild steel conservation in 1 M HCl medium, Chem. Data Collect. 2021; 31, 100638.

35. Obi-Egbedi, N.O. Essien, K.E. Obot, I.B. Ebenso, E.E. 1, 2-Diaminoanthraquinone as corrosion inhibitor for mild steel in hydrochloric acid: weight loss and quantum chemical study, Int. J. Electrochem. Sci. 2011; 6, 913–930.

36. Abd El Rehim, S.S. Ibrahim, M.A.M. Khalid, K.F. The inhibition of 4-(2′-amino-5′-methylphenylazo) antipyrine on corrosion of mild steel in HCl solution, Mater. Chem. Phys. 2001; 70, 268–273. https://doi.org/10.1016/S0254-0584(00)00462-4.

37. Soltani, N. Tavakkoli, N. Kashani, M.K. Mosavizadeh, A. Oguzie, E.E. Jalali, M.R. Silybum marianum extract as a natural source inhibitor for 304 stainless steel corrosion in 1.0 M HCl, J. Ind. Eng. Chem. 2014; 20 3217–3227. https://doi.org/10.1016/j.jiec.2013.12.002.

38. Emranuzzaman, T. Kumar, S. Vishwanatham, G. U. Synergistic effects of formaldehyde and alcoholic extract of plant leaves for protection of N80 steel in 15% HCl, Corros. Eng. Sci. Technol. 2004; 39, 327–332. https://doi.org/10.1179/174327804X13181.

39. Li, X. Deng, S. Xie, X. Fu, H. Inhibition effect of bamboo leaves' extract on steel and zinc in citric acid solution, Corros. Sci. 2014; 87, 15–26. https://doi.org/10.1016/j.corsci.2014.05.013.

40. Eddy, N.O. Experimental and theoretical studies on some amino acids and their potential activity as inhibitors for the corrosion of mild steel, part 2, J. Adv. Res. 2011; 2 35–47. https://doi.org/10.1016/j.jare.2010.08.005.

41. Yadav, M. Behera, D. Kumar, S. Experimental and theoretical studies on corrosion inhibition of mild steel in hydrochloric acid by thiosemicarbazone of Schiff bases, Can. Metall. Q. 2014; 53, 220–231. https://doi.org/10.1179/1879139513Y.0000000118.

42. Deng, S. Li, X. Xie, X. Hydroxymethyl urea and 1, 3-bis (hydroxymethyl) urea as corrosion inhibitors for steel in HCl solution, Corros. Sci. 2014; 80, 276–289. https://doi.org/10.1016/j.corsci.2013.11.041.

43. Obot, A.S. BoEKOM, E.J. ITUEN, E.B. UGI, B.U. ESSIEN, K.E. JONAH, N.B. THERMODYNAMIC INVESTIGATION AND QUANTUM CHEMICAL EVALUATION OF n-HEXANE EXTRACTS OF Costus lucanusianus AS CORROSION INHIBITORS FOR MILD STEEL AND ALUMINUM IN 1 M HCl SOLUTION, J. Appl. Phys. Sci. Int. 2021; 13, 6–27.

44. Eddy, N.O. Part 3. Theoretical study on some amino acids and their potential activity as corrosion inhibitors for mild steel in HCl, Mol. Simul. 2010; 36, 354–363. https://doi.org/10.1080/08927020903483270.

45. Misawa, T. Asami, K. Hashimoto, K. Shimodaira, S.The mechanism of atmospheric rusting and the protective amorphous rust on low alloy steel, Corros. Sci. 1974; 14, 279–289.

46. Misawa, T. Kyuno, T. Suetaka, W. Shimodaira, S. The mechanism of atmospheric rusting and the effect of Cu and P on the rust formation of low alloy steels, Corros. Sci. 1971; 11, 35–48.

47. Ganesan, A.R. Subramani, K. Shanmugam, M. Seedevi, P. Park, S. Alfarhan, A.H. Rajagopal, R. Balasubramanian, B. A comparison of nutritional value of underexploited edible seaweeds with recommended dietary allowances, J. King Saud Univ. 2020; 32, 1206–1211.

48. Ishii, M. Nakahira, M. Yamanaka, T. Infrared absorption spectra and cation distributions in $(Mn, Fe)_3O_4$, Solid State Commun. 1972; 11, 209–212.

49. Ikot, A. N. Akpabio, L. E. Essien, K. Ituen E. E. Obot. I. B. Variational Principle Techniques and the Properties of a Cut-off and Anharmonic Wave Function, E-Journal of Chemistry, 2009; 6(1), 113-119.